# Semiempirical Molecular Orbital Considerations of the Electronic Structures of Transition Metal Complexes. II. Acetylene- and Azo-Nickel Complexes

Kazuyuki Tatsumi, Takayuki Fueno, Akira Nakamura, and Sei Otsuka

*Department of Chemistry, Faculty of Engineering Science, Osaka University, Toyonaka, Osaka 560*

(Received December 22, 1976)

The electronic structures of zerovalent nickel π complexes, $Ni(HC{\equiv}CH)(HNC)_2$ and Ni(*trans*-HN=NH)$(HNC)_2$, have been investigated by the INDO method. Both complexes are found to favor the square-planar geometry, in accord with the observed structures of $Ni(C_6H_5C{\equiv}CC_6H_5)$(*t*-BuNC)$_2$ and $Ni(C_6H_5N{=}NC_6H_5)$(*t*-BuNC)$_2$. Ni(*trans*-HN=NH)$(HNC)_2$ is predicted to be more stable than Ni(*cis*-HN=NH)$(HNC)_2$. The increment in the C–C and N–N bond lengths effected by the complexation seems to well reflect the net effects of σ donation and π back-donation. For the isocyanide N–C bond, an approximately linear relationship is found to hold between the calculated bond index and the observed force constant. It is suggested that both the Ni–C(of acetylene) and Ni–N(of diimide) bondings tend to have greater covalent bond strengths as the electron-releasing ability of the isocyanide ligand increases.

Since the discovery of Zeise's salt, transition metal π complexes have constituted an enormous, diversified field of chemistry.[1] Although the chemistry is well developed, theoretical inquiries to the field have still been limited to olefin complexes.[2] There have been very few attempts at coherent quantum-mechanical description of other π complexes.[3]

In our previous work,[4] we investigated the electronic structure of side-on coordinated nickel dioxygen complex $Ni(O_2)(HNC)_2$ by a modified INDO method. It was found that the greater the extent of back-donation of electrons from Ni to $O_2$, the weaker is the $Ni–O_2$ covalent bond strength. A unique substituent effect was predicted that *both* the $Ni–O_2$ and O–O bondings tend to have greater covalent bond strengths as the electron-attracting ability of the ligand isocyanide increases.

In this paper we will deal with the side-on isocyanide nickel complexes $Ni(HC{\equiv}CH)(HNC)_2$ and Ni(HN=NH)$(HNC)_2$ as model compounds for $Ni(C_6H_5C{\equiv}CC_6H_5)$-(*t*-BuNC)$_2$,[5] and $Ni(C_6H_5N{=}NC_6H_5)$(*t*-BuNC)$_2$,[6] respectively. The purpose of the present study is to clarify the nature of the bondings involved in these complexes and the effects of their geometry and ligand structure on the bondings. A particular attention will be directed to comparisons between these complexes with a dioxygen nickel isocyanide complex, $Ni(O_2)(HNC)_2$.

## Method of Calculation

The same ASMO SCF method at the level of the INDO approximation as described previously[4,7] was used. The basis set of atomic orbitals adopted in the calculation is: 3d, 4s, and 4p for Ni; 2s and 2p for both C and N; and 1s for H. The single-parameter functions of Zerner and Gouterman[8] have been used for the nickel atom while Clementi's functions[9] for ligand atoms. All the one-center integral parameters involved are the same as those used in our earlier paper.[4]

In calculating the core-core repulsion energy $E_{AB}$(core) between atoms A and B, we have used the following function:

$$E_{AB}(\text{core}) = (1-c)\sum_{A}\sum_{B}\sum_{\mu}^{A}\sum_{\nu}^{B}N_{\mu}N_{\nu}(\mu\mu|\nu\nu) + c\sum_{A}\sum_{B}\frac{14.399Z_AZ_B}{R_{AB}} \tag{1}$$

where $N_\mu$ and $N_\nu$ refer to the numbers of the valence electrons occupying AO's $\mu$ and $\nu$, respectively; $(\mu\mu|\nu\nu)$ is the two-center repulsion integral; $Z_A$ and $Z_B$ are the core charge on atoms; and $R_{AB}$ is the internuclear distance between A and B in units of Å. The parameter $c$ has been determined to reproduce the experimental C–C bond length of acetylene (1.203 Å).[10] The resulting $c$ value was 0.353.

## Results and Discussion

*A. Structure of Complexes.* Precise structural information based on the X-ray data is available for $Ni(C_6H_5C{\equiv}CC_6H_5)$(*t*-BuNC)$_2$[11] and Ni(*trans*-$C_6H_5N{=}NC_6H_5$)(*t*-BuNC)$_2$.[12] The dihedral angles θ between the bisisocyanide-nickel plane and the Ni–C–C (of acetylne) and Ni–N–N (of azobenzene) planes are 2.6°(7) and 1.2°(3), respectively, so that the complexes possess essentially the $C_{2v}$ or $C_2$ symmetry. Acetylene, which is linear in the free state, takes a *cis*-bent structure ($\delta = 31.4°$) in the complex. Similarly, for the π-bonded azobenzene complex, there is a dihedral angle of $2\omega = 26.8°$ between the two N–N–C (of phenyl) planes. This angle would be 0° if the C–N–N–C portion of the complex were coplanar as it is in free *trans*-azobenzene.

*Conformation of the Complexes.* In the first place, we will consider the conformations of our model compounds $Ni(HC{\equiv}CH)(HNC)_2$ and Ni(HN=NH)$(HNC)_2$. Calculations were carried out for a few extreme geometries of each compound. Figure 1 illustrates such geometries which can be characterized by two angles, θ and either δ or ω.

The total energies of $Ni(HC{\equiv}CH)(HNC)_2$ for three distinct conformations characterized by the symbol (θ, δ) are presented in Table 1, together with the bond indices $W$[13] for the Ni–C (of acetylene) and C–C bonds, the net charge $Q$ on the acetylene moiety, and the electron populations $q$[4] in the acetylene π and π* orbitals perpendicular (⊥) and parallel (||) to the

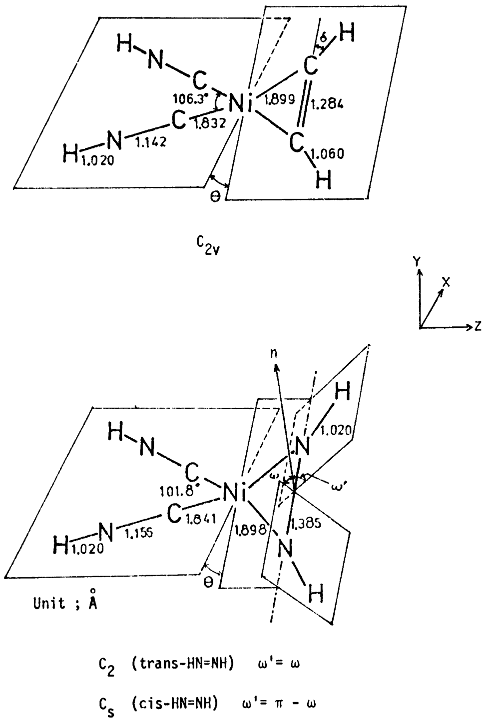

Fig. 1. Coordinate system and structures for Ni(HC≡CH)(HNC)$_2$ and Ni(HN=NH)(HNC)$_2$. The arrow n indicates the direction of the normal line on the plane which the nickel and diimide nitrogens are placed on.

Ni-acetylene plane.[14] Similar sets of data for conformations (θ, ω) of Ni(*trans*-HN=NH)(HNC)$_2$ are given in Table 2.

As can be seen in Tables 1 and 2, the square-planar bent ($\theta=0°$, $\delta>0°$) or twisted ($\theta=0°$, $\omega>0°$) form is more stable than either of the square-planar nonbent ($\theta=\delta=0°$) or untwisted ($\theta=\omega=0°$) structure and the pseudotetrahedral conformation ($\theta=90°$). The results agree well with the X-ray structures of Ni($C_6H_5C\equiv CC_6H_5$)(*t*-BuNC)$_2$ and Ni(*trans*-$C_6H_5N=NC_6H_5$)(*t*-BuNC)$_2$.

The bond indices *W* for the Ni–C (of acetylene) and Ni–N (of diimide) bonds are the greatest for the square-planar bent (or twisted) structure. Since *W* can be regarded as a measure of covalent bond strength of the bond in question,[15] the greatest stability of the form may be ascribable to the greatest covalent character of the Ni–C or Ni–N bond. On the other hand, both $W_{\text{C–C}}$ and $W_{\text{N–N}}$ are the smallest for the square-planar bent and twisted structures. A stronger nickel-acetylene (or diimide) bonding is thus accompanied by a weaker C–C (or N–N) bond. A similar trend is noted in olefin complexes.[16]

Table 1. Total energy (*E*), bond indices (*W*), net charge on acetylene (*Q*), and various orbital populations (*q*) for Ni(HC≡CH)(HNC)$_2$

| (θ, δ) | Square-Planar Bent (0°, 31.4°) | Square-Planar Nonbent (0°, 0°) | Pseudo-tetrahedral Bent (90°, 31.4°) |
|---|---|---|---|
| *E*(eV) | −1424.097 | −1417.332 | −1422.003 |
| $W_{\text{Ni–C}}$ | 0.8183 | 0.6949 | 0.7379 |
| $W_{\text{C–C}}$ | 2.0838 | 2.2465 | 2.1702 |
| $Q_{\text{HC≡CH}}$ | −0.1421 | −0.0080 | −0.1993 |
| $q(\pi_u(\perp))$ | 1.8630 | 1.8786 | 1.9557 |
| $q(\pi_g^*(\perp))$ | 0.0043 | 0.0072 | 0.0021 |
| $q(\pi_u(\parallel))$ | 1.6987 | 1.8618 | 1.6839 |
| $q(\pi_g^*(\parallel))$ | 0.6329 | 0.4865 | 0.6313 |

We now attempt a more detailed analysis of the covalent bond strength of the Ni–C (of acetylene) and Ni–N (of diimide) bonds. Let us first discuss the problem of square-planar *vs.* pseudotetrahedral orientations of acetylene (bent) and diimide (twisted). As shown in Table 1, the net charge on the acetylene $Q_{\text{HC≡CH}}$ is smaller for the former structure. This has arisen primarily from the smaller value of $q(\pi_u(\perp))$, which implies a greater extent of electron donation from acetylene to nickel. To the contrary, the net charge on the diimide $Q_{\text{HN=NH}}$ is greater for the square-planar bent structure (Table 2). The increment of $Q_{\text{HN=NH}}$ has resulted mainly from the greater $q(\pi_g^*(\parallel))$ value,

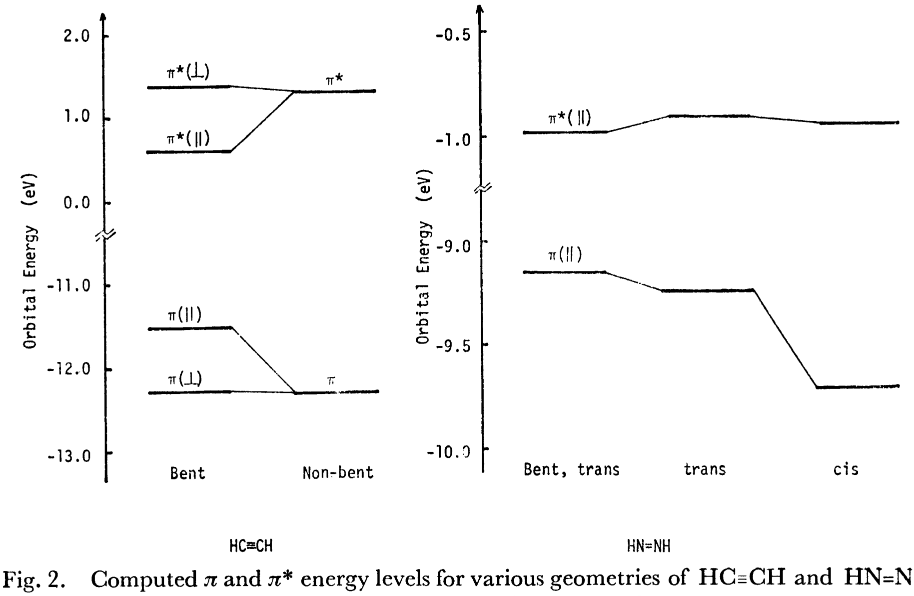

Fig. 2. Computed π and π* energy levels for various geometries of HC≡CH and HN=NH. Bond lengths and angles are the same as those in the complexes.

TABLE 2. TOTAL ENERGY ($E$), BOND INDICES ($W$), NET CHARGE ON DIIMIDE ($Q$), AND $\pi$ ORBITAL POPULATIONS ($q$) FOR Ni(*trans*-HN=NH)(HNC)$_2$ AND Ni(*cis*-HN=NH)(HNC)$_2$

| | *trans*-HN=NH | | | *cis*-HN=NH |
|---|---|---|---|---|
| ($\theta$, $\omega$) | Square-Planar | | Pseudo-tetrahedral | Square-Planar |
| | Twisted (0°, 13.4°) | Untwisted (0°, 0°) | Twisted (30°, 13.4°) | (0°, 13.4°) |
| $E$(eV) | −1515.275 | −1513.445 | −1515.243 | −1515.049 |
| $W_{\text{Ni-N}}$ | 0.8547 | 0.8338 | 0.8382 | 0.8476 |
| $W_{\text{N-N}}$ | 1.1735 | 1.2059 | 1.1854 | 1.1762 |
| $Q_{\text{HN=NH}}$ | −0.3982 | −0.3637 | −0.3888 | −0.3974 |
| $q(\pi_u(\parallel))$ | 1.8057 | 1.8493 | 1.8023 | 1.8131 |
| $q(\pi_g^*(\parallel))$ | 0.9367 | 0.9021 | 0.9078 | 0.9293 |

indicative of a greater extent of back-donation from nickel to diimide. Since a metal-unsaturated ligand bonding is accomplished by two independent interactions, $\sigma$ donation and $\pi$ back-donation, the greater extent of either process would strengthen the bond. Thus, the covalency of both the Ni–(HC≡CH) and Ni–(HN=NH) bonds is greater for the square-planar bent form as has been concluded on the basis of the bond index. However, it is noteworthy here that the origins of the greater stabilities for the square-planar forms differ between the acetylene- and azo-nickel complexes.

Next, we examine the bending ($\delta$) and twisting ($\omega$) effects of acetylene and diimide on the metal–$\pi$ ligand bondings. Comparisons are now made between two extreme geometries, the square-planar bent ($\delta,\omega > 0°$) and the square-planar nonbent ($\delta,\omega = 0°$) structures. Both $q(\pi_u(\perp))$ and $q(\pi_u(\parallel))$ of the acetylene complex decrease in magnitude as the acetylene bends, while $q(\pi_g^*(\parallel))$ increases (Table 1). These results indicate greater extents of both $\sigma$ donation and $\pi$ back-donation for the bent form. The greater interaction means a greater Ni–(HC≡CH) bond strengthening. A change in the negligibly small $q(\pi_g^*(\perp))$ value need not be taken into account. In the diimide complex, $q(\pi_u(\parallel))$ is smaller for the twisted form, while $q(\pi_g^*(\parallel))$ is larger (Table 2). Thus the nickel–diimide bonding is also strengthened by the twisting of the diimide skeleton.

What brings about the increases in both the $\sigma$ donation and $\pi$ back-donation in the bent form? A possible answer can be obtained from the comparisons of the $\pi$ and $\pi^*$ orbital energy levels for the isolated HC≡CH and HN=NH fragments between the bent and nonbent structures (Fig. 2). In the case of acetylene, both occupied orbitals $\pi_u(\perp)$ and $\pi_u(\parallel)$ are more or less destabilized by the distortion while the unoccupied $\pi_g^*(\parallel)$ orbital lowers in energy. The destabilization of the occupied orbitals leads to a greater donor ability of the bent form while the stabilization of $\pi_g^*(\parallel)$ results in the greater acceptor ability. Contrary to this, the $\pi_g^*(\perp)$ orbital rises in energy as acetylene bends. However, this effect hardly exerts influence on the Ni–C (of acetylene) bonding because of the small overlap between Ni $d_{xy}$ and C $p_y$ orbitals (0.019). The diimide $\pi_u(\parallel)$ and $\pi_g^*(\parallel)$ orbitals show the same tendency as those of acetylene. The greater $\sigma$ donor and $\pi$ acceptor abilities of the twisted diimide can thus likewise be accounted for.

*Configuration of HN=NH.* For azo compounds two possible geometrical isomers, *cis* and *trans*, exist. We will focus our attention on the relative stabilities of the azo nickel complexes formed from the *cis* and *trans* isomers of HN=NH. We have calculated the total energy of our model compound Ni(*cis*-HN=NH)(HNC)$_2$, in which the bond lengths and angles are taken to be the same as those in *trans*-HN=NH complex. The result is given in the final column of Table 2, together with the bond indices $W$ for the Ni–N and N–N bonds as well as the $\pi$ and $\pi^*$ orbital populations.

As Table 2 shows, the *trans* azo complex (square-planar bent) is more stable than the *cis*. The result may endorse the fact that the catalysis with low-valent diamagnetic metal complexes leads only to the *cis*→*trans* isomerization of *cis*-azobenzene; the reverse catalytic process hardly takes place.[17]

The greater stability of the *trans*-diimide complex as compared with the complex of the *cis* isomer is wholly compatible with the foregoing arguments on the effects of ligand deformation. Thus, the bond index $W_{\text{Ni-N}}$ is larger in the *trans* isomer, indicative of a greater covalent character of the Ni–N bond. The $\pi$ orbital population $q(\pi_u(\parallel))$ of the *trans*-diimide complex is smaller than that of the *cis* complex, while $q(\pi_g^*(\parallel))$ is greater in the former. The greater stability of the *trans* isomer would thus be a consequence of the greater extents of $\sigma$ donation and $\pi$ back-donation, which could immediately be rationalized from the $\pi$ orbital level diagram shown in Fig. 2.

### *B. Ni-Ligand Bondings in the Square-Planar Conformer.*

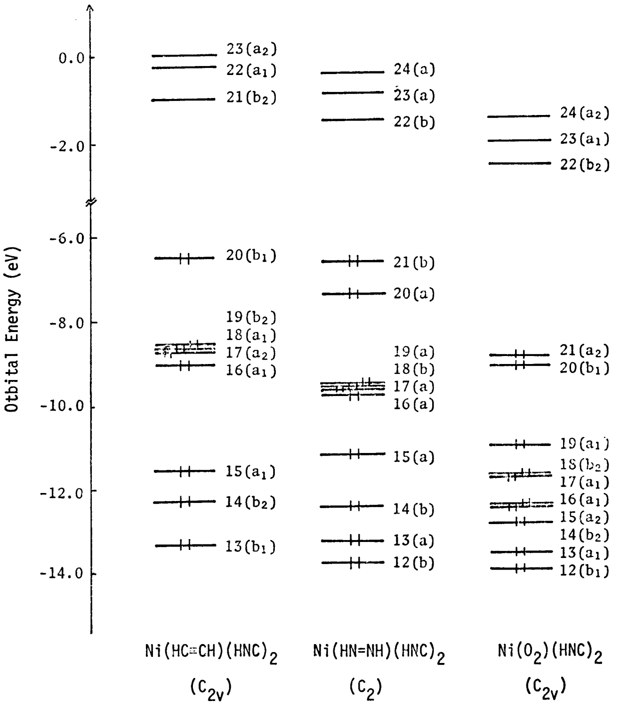

Fig. 3. Upper portions of the molecular orbital level diagrams for Ni(HC≡CH)(HNC)$_2$, Ni(HN=NH)(HNC)$_2$, and Ni(O$_2$)(HNC)$_2$. The highest occupied levels are 20 ($b_1$), 21(b), and 21($a_2$), respectively.

In this section, we will describe the electronic structure of $Ni(HC{\equiv}CH)(HNC)_2$ and $Ni(\textit{trans}\text{-}HN{=}NH)(HNC)_2$[18] for the square-planar form in detail. The level height and form of the bonding molecular orbitals are our specific concern here.

*Molecular Orbitals.* The molecular orbital energy levels are diagrammatically shown in Fig. 3, where those for the dioxygen complex $Ni(O_2)(HNC)_2$ are also shown for the sake of comparison. The levels are labeled according to the irreducible representations of the $C_{2v}$ point group, except for the *trans*-diimide complex of the $C_2$ point group. Only the low-lying vacant orbitals and the upper portion of the occupied orbitals are included in the diagrams; lower orbitals which have been omitted in the diagrams consist merely of the essentially unperturbed ligand orbitals lying in the range $-44.8$ to $-15.5$ eV.

The lowest unoccupied levels, $\phi_{21}(b_2)$ for the acetylene complex and $\phi_{22}(b)$ for the azo complex, consist primarily of the isocyanide $\pi^*(\perp)$ orbital with an appreciable Ni $4p_y$ character. The highest occupied level $\phi_{20}(b_1)$ for the former complex is an admixture of the Ni $3d_{xz}$ with the $HC{\equiv}CH$ $\pi_g^*(\parallel)$ orbital. Similarly, $\phi_{21}(b)$ for the latter involves the mixing between the Ni $3d_{xz}$ and $HN{=}NH$ $\pi_g^*(\parallel)$ orbitals. These two bonding orbitals are of back-donation type which contribute to the Ni–($HC{\equiv}CH$) or Ni–($HN{=}NH$) bonding, corresponding to $\phi_{20}(b_1)$ for the dioxygen complex. Incidentally, the orbital $\phi_{21}(a_2)$ of the dioxygen complex is the lone-pair orbital $\pi_g^*(\perp)$ of $O_2$.

It is clear from Fig. 3 that the $\pi$-type bonding orbitals ascribable to the back-donation are more stabilized with the increase in the $\pi$ acceptor ability of the unsaturated ligands. Figure 4 shows the contour maps of these back-donation type orbitals. The maps clearly show the delocalization of electrons from the Ni $3d_{xz}$ into the ligand $\pi_g^*(\parallel)$ orbital, which increases in the order $HC{\equiv}CH<HN{=}NH<O_2$, in harmony with the decreasing order of the $\pi^*$ energy levels of the free molecules; 1.910 eV ($HC{\equiv}CH$), 0.014 eV ($HN{=}NH$), and $-12.05$ eV ($O_2$).[19]

The Ni–($HC{\equiv}CH$) and Ni–($HN{=}NH$) $\sigma$-type bondings are accomplished through donation type orbitals such as $\phi_{15}(a_1)$, $\phi_{16}(a_1)$, and $\phi_{18}(a_1)$ for the former complex and $\phi_{15}(a)$, $\phi_{16}(a)$, and $\phi_{19}(a)$ for the latter. However, each level is found to involve relatively small mixings between the Ni $d_{x^2-y^2}$ and $d_{z^2}$ orbitals with the ligand $\pi_u(\parallel)$ orbital as compared to the back-donation type orbital.

All these results imply the relative importance of the $\pi$-type bonding in such basic zerovalent nickel complexes. Consistently, chemical and spectroscopic informations of zerovalent nickel olefin complexes show a considerable back-donation from nickel d to olefin $\pi^*$ orbital.[21–24] The stability of the complexes is even governed entirely by the amount of back-donation.[23c,25] The trend forms a sharp contrast with the relative importance of $\sigma$ donation in Zeise's anion $[Pt(C_2H_4)Cl_3]^-$ [26] as well as silver(I)-olefin complexes.[27]

Another type of Ni–($HC{\equiv}CH$) bonding is accomplished through the mixing of the $HC{\equiv}CH$ $\pi_u(\perp)$ orbital with the Ni $d_{yz}$ orbital in $\phi_{14}(b_2)$. This is compatible with the model presented for platinum acetylene complexes by Nelson *et al.*[3a] A similar identification can be made for the dioxygen complex in the level $\phi_{14}(b_2)$.[4] The corresponding levels for the

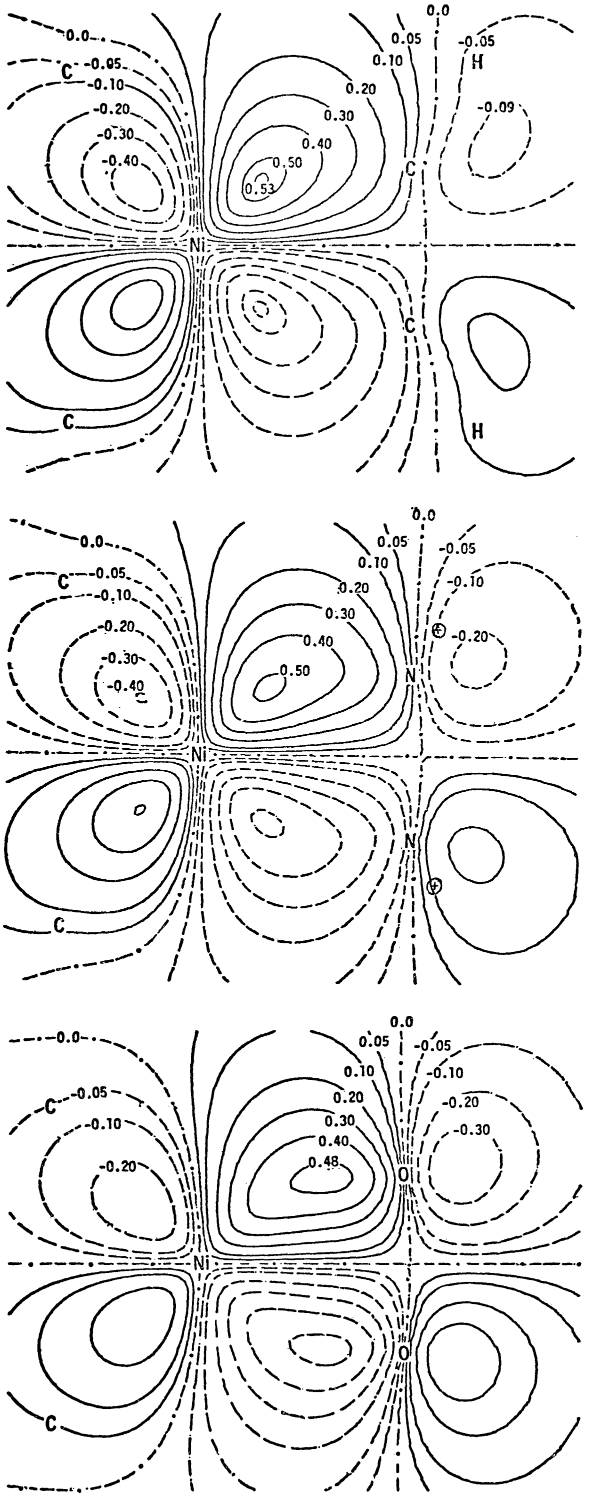

Fig. 4. Contour plots of the $\pi$-like bonding orbitals of (A) $Ni(HC{\equiv}CH)(HNC)_2$ [$20b_1$], (B) $Ni(HN{=}NH)(HNC)_2$ [$21b$], and (C) $Ni(O_2)(HNC)_2$ [$20b_1$]. The nitrogen and hydrogen atoms of the isocyanide ligand are excluded in the plots. The points marked with ⊕ are the projections of the hydrogen atoms onto the xz plane.

azo complex are $\psi_{20}$(a) and $\psi_{14}$(b), which are the combinations of the two lone-pair orbitals on diimide. The mixing of the lone-pair with Ni d orbitals is practically zero.

*Charge Distribution.* Table 3 summarizes the calculated distributions of valence electrons over the nickel s, p, and d orbitals as well as the ligand atoms in the complexes. According to these results, the apparent electronic configurations of nickel are $(3d)^{8.90}(4s)^{0.52}(4p)^{1.07}$, $(3d)^{8.80}(4s)^{0.53}(4p)^{0.99}$, and $(3d)^{8.49}(4s)^{0.54}(4p)^{0.98}$ for $\mathrm{Ni(HC{\equiv}CH)(HNC)_2}$, $\mathrm{Ni(HN{=}NH)(HNC)_2}$, and $\mathrm{Ni(O_2)(HNC)_2}$, respectively. The net charge density on the nickel atom ranges from $-0.49$ to $-0.01$, increasing in the order $\mathrm{Ni(HC{\equiv}CH)(HNC)_2} < \mathrm{Ni(HN{=}NH)(HNC)_2} < \mathrm{Ni(O_2)(HNC)_2}$. Their total d orbital occupation numbers lie between 8 and 9 and tend to increase in the reverse order. These trends are governed almost exclusively by the population on the $d_{xz}$ orbital; nearly two electrons keep residing in each of the remaining four d orbitals. The above-mentioned order can be anticipated from the electronegativities of acetylene, diimide, and dioxygen. By a similar reasoning, positive charges on the donating isocyanide ligands should increase in the order $\mathrm{Ni(HC{\equiv}CH)(HNC)_2} < \mathrm{Ni(HN{=}NH)(HNC)_2} < \mathrm{Ni(O_2)(HNC)_2}$. The charge transfer from the $\mathrm{Ni(HNC)_2}$ identity to each unsaturated ligand amounts to 0.14 (acetylene), 0.41 (diimide), or 0.88 (dioxygen) of an electron.

TABLE 3. CALCULATED ELECTRON DISTRIBUTIONS FOR $\mathrm{Ni(C_2H_2)(HNC)_2}$, $\mathrm{Ni(N_2H_2)(HNC)_2}$, AND $\mathrm{Ni(O_2)(HNC)_2}$

| Atom | Atomic orbital | Charge density | | |
|---|---|---|---|---|
| | | $\mathrm{Ni(C_2H_2)\text{-}(HNC)_2}$ | $\mathrm{Ni(N_2H_2)\text{-}(HNC)_2}$ | $\mathrm{Ni(O_2)\text{-}(HNC)_2}$ |
| Ni | s | 0.517 | 0.529 | 0.537 |
| | p | 1.065 | 0.991 | 0.975 |
| | $d_{xz}$ | 1.151 | 0.966 | 0.580 |
| | $d_{yz}$ | 1.928 | 1.957 | 1.978 |
| | $d_{xy}$ | 1.960 | 1.974 | 1.988 |
| | $d_{x^2-y^2}$ | 1.951 | 1.965 | 1.982 |
| | $d_{z^2}$ | 1.912 | 1.933 | 1.959 |
| C(C≡C) | s, p | 4.155 | | |
| H | s | 0.916 | | |
| N(N=N) | s, p | | 5.348 | |
| H | s | | 0.851 | |
| O(O=O) | s, p | | | 6.437 |
| C(CNH) | s, p | 3.921 | 3.897 | 3.860 |
| N | s, p | 4.964 | 4.953 | 4.923 |
| H | s | 0.801 | 0.794 | 0.780 |

*C. Bondings within the Ligands.* The activation of unsaturated ligands by metal complexes has received considerable attention because of possible catalytic applications.[28,29] We will elaborate, in this section, on the properties of C≡C and N=N bondings as well as the isocyanide C≡N bond in the complexes.

*The C≡C and N=N Bondings.* In Table 4, the various $\pi$ orbital populations for the acetylene and diimide complexes in the most stable forms are compared with those for free acetylene and diimide. The electron donation from nickel to the organic moiety upon complexation is reflected in the diminution in $q(\pi_u(\perp))$ or $q(\pi_u(\|))$ while the back-donation, in the increment in $q(\pi_g^*(\|))$. The following points are noteworthy in Table 4: (1) The back-donation to the acetylene $\pi_g^*(\perp)$ orbital is almost zero, in contrast to an appreciable donation from the acetylene $\pi_u(\perp)$ orbital; (2) despite the presence of the filled lone-pair orbitals, diimide acts as a fairly efficient $\pi$ acceptor toward zerovalent nickel; and (3) the total $\pi$ population in each complex is greater than that in the corresponding free unsaturated ligand. At any rate, both the diminution in $q(\pi_u)$ and the enhancement in $q(\pi_g^*)$ should lead to loosening of the C≡C and N=N bonds.

TABLE 4. CALCULATED ORBITAL POPULATIONS ($q$) AND OBSERVED BOND LENGTH ($R$)

| | $\mathrm{Ni(C_2H_2)\text{-}(HNC)_2}$ | $\mathrm{C_2H_2}$ | $\mathrm{Ni(N_2H_2)\text{-}(HNC)_2}$ | $\mathrm{N_2H_2}$ |
|---|---|---|---|---|
| $q(\pi_u(\perp))$ | 1.86 | 2.00 | — | — |
| $q(\pi_u(\|)$ | 1.70 | 2.00 | 1.81 | 2.00 |
| $q(\pi_g^*(\perp))$ | 0.00 | 0.00 | — | — |
| $q(\pi_g^*(\|)$ | 0.63 | 0.00 | 0.94 | 0.00 |
| $\Delta q$ | 2.92 | 4.00 | 0.87 | 2.00 |
| $R_{L-L}$(Å) | 1.284[a)] | 1.19[b)] | 1.385[c)] | 1.243[d)] |

a) For $\mathrm{Ni(C_6H_5C{\equiv}CC_6H_5)(\mathit{t}\text{-}BuNC)_2}$, Ref. 11. b) For $\mathrm{C_6H_5C{\equiv}CC_6H_5}$, J.M. Robertson and I. Woodward, *Proc. R. Soc., Ser. A*, **164**, 436 (1938). c) For $\mathrm{Ni(C_6H_5N{=}NC_6H_5)(\mathit{t}\text{-}BuNC)_2}$, Ref. 12. d) For $\mathrm{C_6H_5N{=}NC_6H_5}$, C. J. Brown, *Acta Crystallogr.*, **21**, 146 (1966).

We have previously introduced the quantity[4)]

$$\Delta q = q(\pi_u(\perp)) + q(\pi_u(\|)) - q(\pi_g^*(\perp)) - q(\pi_g^*(\|)) \quad (2)$$

as a measure of the strength of the O–O $\pi$ bond in the nickel dioxygen complex. The values of $\Delta q$ calculated for HC≡CH and HN=NH, both complexed and uncomplexed, are included in Table 4. For either of the acetylene and azo complexes studied, $\Delta q$ is much smaller than that for the corresponding free substrate. This would effect a considerable increase in the C≡C as well as N=N bond length $R$, as is actually the case.

The above-stated trend could be cast into a more quantitative generalization,[30,31)] since conceptually our $\Delta q$ is twice the $\pi$-bond order of the unsaturated ligand. Thus we consider the ratio of the increase in $R$ upon complexation to that brought about on going from an unsaturated bond to a saturated one:[32)]

$$r = \frac{R_{L=L}(\text{complex}) - R_{L=L}(\text{free})}{R_{L-L}(\text{saturated}) - R_{L=L}(\text{free})} \quad (3)$$

$$L = \mathrm{C, N, and\ O}$$

The ratio $r$ is now to be compared with the change in $\Delta q$ effected by complexation:

$$\Delta(\Delta q) = \Delta q(\text{complex}) - \Delta q(\text{free}) \quad (4)$$

The $\Delta(\Delta q)$ takes on a value $-2$ when complexation involves a complete destruction of a $\pi$ bond of the ligand. Needless to say, $\Delta(\Delta q) = 0$ when complexation does not take place. The ratio $r$ should respectively be 1 and 0 in these extreme cases.

Figure 5 is the plots of $r$ against $\Delta(\Delta q)$ for the nickel isocyanide complexes of acetylene, diimide, dioxygen,

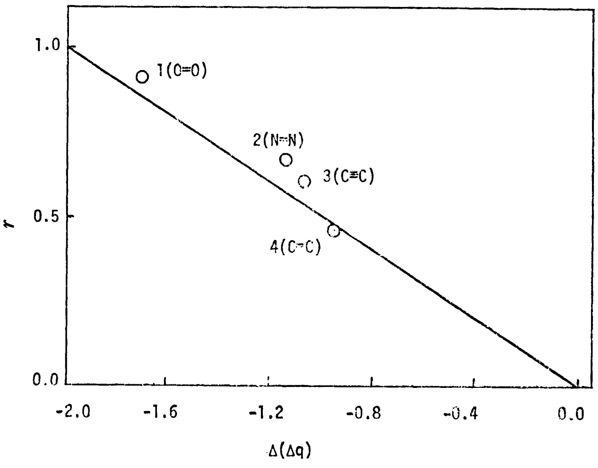

Fig. 5. Plots of the bond length ratio $r$ of nickel complexes against the $\Delta(\Delta q)$ values calculated for the corresponding model compounds:
(1) $Ni(O_2)(t\text{-}BuNC)_2$
(2) $Ni(trans\text{-}C_6H_5N{=}NC_6H_5)(t\text{-}BuNC)_2$
(3) $Ni(C_6H_5C{\equiv}CC_6H_5)(t\text{-}BuNC)_2$
(4) $Ni(H_2C{=}CH_2)(P(C_6H_5)_3)_2$
The model compounds assumed are $Ni(O_2)(HNC)_2$, $Ni(trans\text{-}HN{=}NH)(HNC)_2$, $Ni(HC{\equiv}CH)(HNC)_2$, and $Ni(H_2C{=}CH_2)(PH_3)_2$, respectively. The bond length of $O_2$ in $Ni(O_2)(t\text{-}BuNC)_2$ was taken from M. Matsumoto and K. Nakatsu, *Acta Crystallogr.*, **B31**, 2711 (1975); for $Ni(H_2C{=}CH_2)(P(C_6H_5)_3)_2$, P.-T. Cheng, C. D. Cook, C. H. Koo, S. C. Nyburg, and M. T. Shimoni, *Acta Crystallogr.*, **B27**, 1904 (1971).

and ethylene. All the plots fall in the vicinity of the straight line which connects the two extreme points mentioned above. The results would make such plots for different atomic pairs meaningful.

*N≡C Bonding.* Infrared study[33] of a series of *cis*-planar nickel bisisocyanide complexes concludes that they possess two N≡C stretching bands assignable to the a and b modes with respect to the $C_2$ point group. We have applied the method of Cotton and Kraihanzel[34,35] to the two stretching frequencies observed, to derive a set of approximate force constants $f_{N-C}$ and $f_i$. The former is the N≡C stretching force constant while the latter represents the *cis*-type (N≡C stretch)-(N≡C stretch) vibrational interaction force constant. Although there are several well-founded criticisms of the method,[36,37] it still seems to be useful for a comparative study of a family of analogous compounds.[38]

We here consider the N≡C stretching force constant $f_{N-C}$. Plotted in Fig. 6 are the $f_{N-C}$ values for $Ni(C_6H_5C{\equiv}CC_6H_5)(t\text{-}BuNC)_2$, $Ni(C_6H_5N{=}NC_6H_5)(t\text{-}BuNC)_2$, and $Ni(O_2)(t\text{-}BuNC)_2$ against the bond indices $W_{N-C}$ calculated for the N≡C bond of the corresponding model compounds. As can be seen in Fig. 6, there is a reasonably good linearity between $f_{N-C}$ and $W_{N-C}$ with a positive slope.

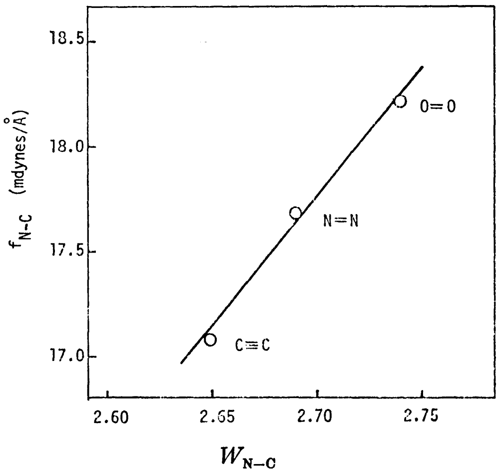

Fig. 6. Plots of the N≡C stretching force constants ($f_{N-C}$) *vs.* calculated bond indices ($W_{N-C}$) of the corresponding model compounds.

*D. Polar Effect of Isocyanide Substituent.* In dealing with the effects of substituent in isocyanide on the strengths of nickel-ligand bonds and the ligand C≡C and N=N bonds, we employ a similar model as has been used previously.[4)] That is, we assume a hypothetical isocyanide ligand (CNH′, for which the valence-state ionization potential $I_S^H$ for the hydrogen atom H′ is allowed to vary, with the other parameters being fixed. When $I_S^H$ is greater than 13.6 eV, CNH′ should be more electronegative than CNH, and *vice versa*. The differen-

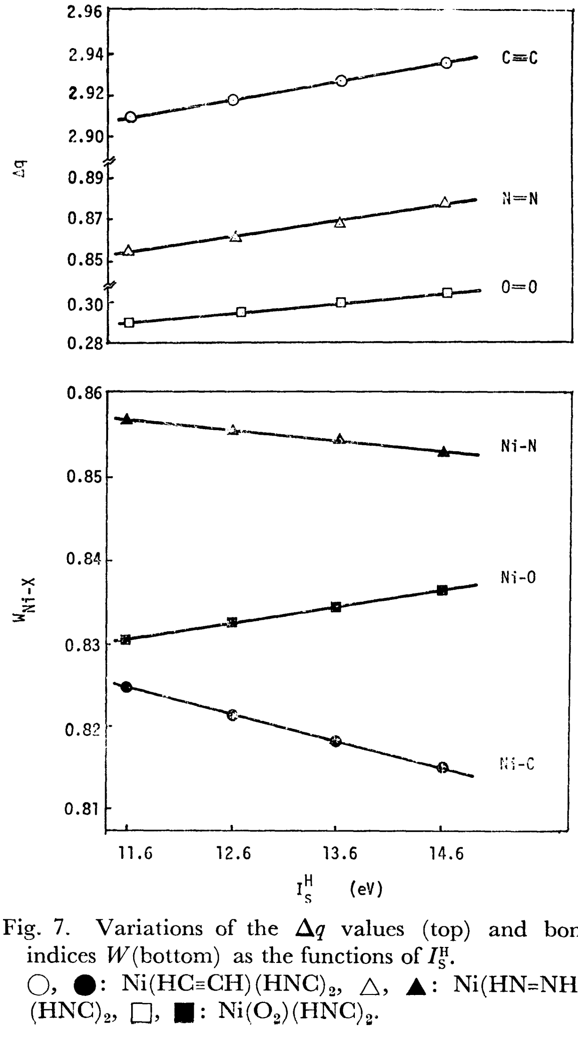

Fig. 7. Variations of the $\Delta q$ values (top) and bond indices $W$(bottom) as the functions of $I_S^H$.
○, ●: $Ni(HC{\equiv}CH)(HNC)_2$, △, ▲: $Ni(HN{=}NH)(HNC)_2$, □, ■: $Ni(O_2)(HNC)_2$.

tial π orbital population $\Delta q$ and bond indices $W$ for the hypothetical complexes $Ni(HC{\equiv}CH)(H'NC)_2$ and $Ni(HN{=}NH)(H'NC)_2$ were calculated by varying $I_{\rm S}^{\rm H}$ from 11.6 to 14.6 eV.

Figure 7 shows the variations in $\Delta q$ and $W_{\rm Ni-L}$ as the functions of $I_{\rm S}^{\rm H}$. For the purpose of comparison, the calculated data for dioxygen complex $Ni(O_2)(H'NC)_2$ are also plotted. As Fig. 7 shows, the $\Delta q$-values for these three complexes altogether increase with the increasing $I_{\rm S}^{\rm H}$. Thus, as the isocyanide ligand becomes more electronegative, all the C≡C, N=N, and O=O bondings should be more and more strengthened. The trend can easily be accounted for in terms of the decreasing back-donation from nickel to the π* orbital(s) of the unsaturated ligands.

As for the strength of the nickel–ligand bonds, both $W_{\rm Ni-C}$ and $W_{\rm Ni-N}$ decrease as the isocyanide ligand becomes more electron-withdrawing. The situation is analogous to the substitution effect on the metal–olefin π-bonding interaction in various olefin complexes.[16] By contrast, the $W_{\rm Ni-O}$ increases as $I_{\rm S}^{\rm H}$ increases. That is, substitution of electronegative ligands tend to increase the nickel–oxygen bond strength.

The unique electronic effects of isocyanide substituents on the Ni–O bond strength can be rationalized from the type of orbital interactions involved. Figure 8 is a schematic level diagram for the highest occupied $b_1$ orbital of $Ni(HNC)_2(C_{2v})$ and the frontier π and π* orbitals of the three isolated molecules, HC≡CH, HN=NH, and $O_2$. For the sake of convenience, the $Ni(HNC)_2$ $b_1$ and $O_2$ π levels are depicted as doubly occupied orbitals, although in reality calculations were performed by the UHF-INDO method. Note that the $b_1$ orbital in question lies below the π* orbitals of HC≡CH and HN=NH but certainly above the π* level of $O_2$.

The $b_1$ orbital which consists mainly of the Ni $3d_{xz}$ orbital interacts with the π* levels, and this interaction contributes most dominantly to the back-donation. As the CNH is replaced by a more electron-releasing ligand, the $b_1$ level will be destabilized accordingly. This destabilization in turn should enhance the abovementioned type of orbital interactions for the cases of HC≡CH and HN=NH whereas it should lead to a diminution in interaction in the case of $O_2$, as will be readily understood by a simple perturbation theory. The situations are wholly compatible with the trends noted in Fig. 7.

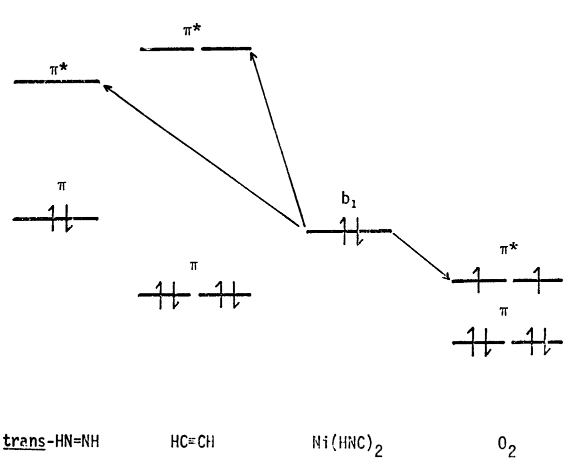

Fig. 8. Schematical level diagrams for the π and π* orbitals of *trans*-HN=NH, HC≡CH, and $O_2$ as well as the highest $b_1$ orbitals of $Ni(HNC)_2$. The back-donation of electrons occurs in the direction of the arrows.

## References

1) For a recent comprehensive review, R. F. Heck, "Organotransition Metal Chemistry," Academic Press, New York and London (1974).

2) a) J. W. Moore, *Acta Chem. Scand.*, **20**, 1154 (1966); b) H. Kato, *Bull. Chem. Soc. Jpn.*, **44**, 348 (1971); c) E. J. Baerends, D. E. Ellis, and R. Ross, *Theor. Chim. Acta (Berlin)*, **27**, 339 (1972); d) K. H. Johnson and F. C. Smith, Jr., *Phys. Rev.*, **B5**, 831 (1972).

3) a) J. H. Nelson, K. S. Wheelock, L. C. Cusacks, and H. B. Jonassen, *J. Am. Chem. Soc.*, **91**, 7005 (1969); *ibid.*, **92**, 5110 (1970); *Inorg. Chem.*, **11**, 422 (1972); *Chem. Commun.*, **1969**, 1019; b) J. G. Norman, Jr., *J. Am. Chem. Soc.*, **96**, 3327 (1974).

4) K. Tatsumi, T. Fueno, A. Nakamura, and S. Otsuka, *Bull. Chem. Soc. Jpn.*, **49**, 2164 (1976).

5) S. Otsuka, T. Yoshida, and Y. Tatsuno, *J. Chem. Soc., D*, **1971**, 42.

6) S. Otsuka, T. Yoshida, and Y. Tatsuno, *Chem. Commun.*, **1971**, 67.

7) K. Tatsumi and T. Fueno, *Bull. Chem. Soc. Jpn.*, **49**, 929 (1976).

8) M. Zerner and M. Gouterman, *Theor. Chim. Acta (Berlin)*, **4**, 44 (1966).

9) E. Clementi and D. L. Raimond, *J. Chem. Phys.*, **38**, 2686 (1963).

10) A. D. Mitchell ed., "Table of Interatomic Distances and Configuration in Molecules and Ions," The Chemical Society, London (1958).

11) R. S. Dickson and J. A. Ibers, *J. Organometal. Chem.*, **36**, 191 (1972).

12) R. Dickson and J. A. Ibers, *J. Am. Chem. Soc.*, **93**, 4636 (1971); *ibid.*, **94**, 2988 (1972).

13) K. B. Wiberg, *Tetrahedron*, **24**, 1083 (1968).

14) Strictly speaking, the π and π* orbitals cannot be extracted from the molecular orbitals of the complexes in which HC≡CH and HN=NH are distorted in structure. However, since the distortion (δ or ω) is small, we may assume that both orbitals are constructed virtually of the $p_z(\parallel)$ and $p_y(\perp)$ (or $p_x(\perp)$) atomic orbitals alone.

15) T. Okada and T. Fueno, *Bull. Chem. Soc. Jpn.*, **48**, 2025 (1975).

16) F. R. Hartly, *Chem. Rev.*, **69**, 799 (1969); *Angew. Chem. Intern. Edit.*, **11**, 596 (1972).

17) A. Nakamura, K. Doi, K. Tatsumi, and S. Otsuka, *J. Mol. Catal.*, in press.

18) Hereafter in this paper, HN=NH denotes only a *trans* diimide unless otherwise noted.

19) These $\pi_g{}^*$ orbital energies of acetylene and diimide were calculated using the INDO method. That of dioxygen was given by the UHF-INDO calculation. Molecular geometries are taken from the literature; see Refs. 10 and 20.

20) N. W. Winter and R. M. Pitzer, *J. Chem. Phys.*, **62**, 1269 (1975).

21) G. N. Schrauzer, *Chem. Ber.*, **94**, 6421 (1961).

22) H. B. Gray and C. J. Ballhausen, "Molecular Orbital Theory," W. A. Benjamin, New York, N. Y. (1964).

23) a) A. Yamamoto and S. Ikeda, *J. Am. Chem. Soc.*, **89**, 5989 (1967); b) A. Yamamoto, T. Shimizu, and S. Ikeda, *Polym. J.*, **1**, 171 (1970); c) T. Yamamoto, A. Yamamoto, and S. Ikeda, *J. Am. Chem. Soc.*, **93**, 3350, 3360 (1971).

24) a) C. A. Tolman, W. C. Seidel, and D. H. Gerlach, *J. Am. Chem. Soc.*, **94**, 2669 (1972); b) C. A. Tolman and W. C. Seidel, *ibid.*, **96**, 2774 (1974).

25) C. A. Tolman, *J. Am. Chem. Soc.*, **96**, 2780 (1974).

26) N. Rösch, R. P. Messmer, and K. H. Johnson, *J. Am. Chem. Soc.*, **96**, 3855 (1974).

27) H. Basch, *J. Chem. Phys.*, **56**, 441 (1972).

28) M. M. T. Khan and A. E. Martell, "Homogeneous Catalysis by Metal Complex," Vol. 1, Academic Press, New York and London (1974).

29) G. H. Olivé and S. Olivé, *Angew. Chem. Internat. Edit.*, **10**, 105 (1971); *ibid.*, **13**, 29 (1974).

30) C. A. Coulson, *Proc. R. Soc., Ser. A*, **169**, 413 (1939).

31) M. J. S. Dewar and H. N. Schmeising, *Tetrahedron*, **5**, 166 (1959); **11**, 96 (1960).

32) In the case of $HC\equiv CH$, the subscripts L–L and L=L should be read as indicating the $C=C$ and $C\equiv C$ bonds, respectively.

33) S. Otsuka, T. Yoshida, and Y. Tatsuno, *J. Am. Chem. Soc.*, **93**, 6462 (1971).

34) F. A. Cotton and C. S. Kraihanzel, *J. Am. Chem. Soc.*, **84**, 4432 (1962).

35) This method has widely been extended to various metal carbonyl and isocyanide systems. See for examples; W. Beck and K. Lottes, *Chem. Ber.*, **98**, 2657 (1965); A. C. Sarapu and R. F. Fenske, *Inorg. Chem.*, **14**, 247 (1975).

36) L. M. Bower and M. H. B. Stiddard, *Inorg. Chim. Acta*, **1**, 231 (1967).

37) L. H. Jones, *Inorg. Chem.*, **7**, 1681 (1968).

38) a) G. R. Van Hecke and W. DeW. Horrocks, Jr., *Inorg. Chem.*, **5**, 1960 (1966); b) F. A. Cotton, *ibid.*, **7**, 1683 (1968).